Lignin-enriched Fermentation Residues from Bioethanol Production of Fast-growing Poplar and Forage Sorghum

José I. Santos,[a] Úrsula Fillat,[b] Raquel Martín-Sampedro,[b] Ignacio Ballesteros,[c] Paloma Manzanares,[c] Mercedes Ballesteros,[c] María E. Eugenio,[b] and David Ibarra [b,*]

The current challenges in developing a cost-effective bioethanol industry include the production of not only high-volume, low cost biofuels but also high-value products with minimal downstream waste. The up-grading of side-stream lignins from bioethanol production plants to novel high-value products will improve the profitability of the bioethanol industry; to do that, a precise understanding of lignin is required. In the present study, lignin-enriched fermentation residues from bioethanol production (steam explosion pretreatment, saccharification, and fermentation) of fast-growing poplar and forage sorghum were characterized. In addition to the purity and composition, lignin structure (syringyl/guaiacyl (S/G) ratio, inter-unit linkages) was also analyzed with spectroscopy techniques such as Fourier transform infrared and two-dimensional nuclear magnetic resonance. Bioethanol processing and feedstock origins seemed to be the main factors determining the purity, composition, and structure of lignins. Residual lignins from poplar and forage sorghum contained significant amounts of sugar and protein impurities. Poplar lignin showed a very high S/G ratio associated with *p*-hydroxybenzoate. A lower S/G ratio together with H lignin units and *p*-hydroxycinnamates (*p*-coumarate and ferulate) was observed for forage sorghum lignin. The main inter-unit linkages present in both lignins were *β-O*-4´ aryl ether followed by resinols and phenylcoumarans.

INTRODUCTION

A competitive, innovative, and sustainable biobased economy can be founded on locally sourced and produced plant and waste-derived fuels, materials, and chemicals. This model, the so-called biorefinery, has the potential to lead the transition towards a post-petroleum society and to mitigate global climate change. In this context, lignocellulosic biomass is the most promising feedstock to be used in biorefineries, due to its low cost and wide distribution, and lignocellulosic bioethanol is one of the most significant product within these biorefineries.

Lignocellulosic materials such as poplar and forage sorghum have been identified as promising feedstocks for bioethanol production. Poplar (*Populus* sp.) is a fast-growing and short-rotation energy crop widely used for the manufacture of paper pulp, pallets, cheap plywood (Christersson 2008), and, most recently, for bioethanol (Negro *et al.* 2003; Ballesteros *et al.* 2004). Forage sorghum (*Sorghum* sp.) includes numerous species of

bioresources.com

grasses commonly used as ensilage in forage/livestock systems (Miron *et al.* 2005), and it has been also recognized as a raw material for bioethanol production (Ballesteros *et al.* 2004; Manzanares *et al.* 2012).

Ethanol production from lignocellulosic biomass by biochemical processing comprises the following steps: pretreatment, enzymatic hydrolysis of cellulose and hemicelluloses, sugar fermentation, separation of lignin residue, and distillation (Tomás-Pejó *et al.* 2008). About 40% of the residual lignin is necessary in order to obtain energy to run the processing plant (Sannigrahi and Ragauskas 2011). The rest of the lignin can be transformed into value-added products, thus enhancing the profitability of the bioethanol industry and biorefinery implementations. Up to now, lignin has been investigated for several industrial applications, such as a phenol substitute in the formulation of phenol-formaldehyde resins, as filler in composites, for surfactant/dispersants additives, and as a source of aromatic compounds to produce bulk and fine chemicals (Ragauskas *et al.* 2014).

Lignin is a complex three-dimensional network built up of *p*-hydroxyphenyl (H), guaiacyl (G), and syringyl (S) phenylpropanoid units, which give rise to a variety of subunits that involve C–C and ether bonds (Martínez *et al.* 2009). Due to the complexity and heterogeneity of lignin, a precise understanding of its structure is needed in order to determine how it behaves in various potential applications. In this sense, spectroscopy techniques such as Fourier transform infrared (FTIR) and two-dimensional nuclear magnetic resonance (2D-NMR) are available to offer a deeper knowledge of lignin structure. FTIR spectroscopy provides indication of the presence of functional groups and lignin units composition (Faix 1991), whereas 2D-NMR can provide information on the structure of the whole macromolecule and direct determination of the different lignin moieties and inter-unit linkages (Ralph *et al.* 1999). The use of these techniques has been largely applied in the analysis of wood and non-wood lignins in nature and processes such as pulp and paper manufacturing (Faix 1991; Ibarra *et al.* 2004, 2007a; del Río *et al.* 2008; Yuan *et al.* 2011; Sun *et al.* 2013).

In this study, the lignin-enriched fermentation residues from bioethanol production of fast-growing poplar and forage sorghum were characterized. In addition to the purity and composition, the lignin structure (S/G ratio, inter-unit linkages) was investigated by spectroscopy techniques such as FTIR and 2D-NMR. The compositional and structural characteristics of the mentioned residual lignins will help to maximize its exploitation to high-value products.

EXPERIMENTAL

Materials

Raw Materials and Pretreatment

Poplar biomass (*Populus* sp.), 5% moisture, was supplied by The Renewable Energies Development Centre at Lubia (Soria, Spain). Forage sorghum biomass (*Sorghum* sp.), 9% moisture, was provided by Instituto Tecnológico Agrario de Castilla y León (León, Spain). Biomass samples were coarsely crushed using a laboratory hammer mill (Retsch, Germany), homogenized, and stored until used. The chemical composition (% dry weight) of poplar and forage sorghum are shown in Table 1.

Steam explosion pretreatment was performed by applying Masonite technology in a small batch plant equipped with a 2-L reaction vessel designed to reach a maximum operating pressure of 4.12 MPa, as described in previous works (Negro *et al.* 2003;

Manzanares *et al.* 2012). After explosion, the materials were recovered in a cyclone, and the wet materials were cooled to about 40 ℃ and filtered for solids recovery. The solid fractions were thoroughly washed to obtain the water-insoluble solid (WIS) fractions. Temperature and residence time conditions of pretreatment for poplar (210 ℃, 4 min) and forage sorghum (220 ℃, 7 min) biomass samples were based on optimal sugars recovery and enzymatic hydrolysis yield (Negro *et al.* 2003; Manzanares *et al.* 2012).

Table 1. Chemical Composition of Fast-growing Poplar and Forage Sorghum

Composition (% dry weight)	Poplar	Forage Sorghum
Cellulose	39.5	35.2
Hemicelluloses	22.0	23.1
Xylan	15.8	20.8
Galactan	2.2	0.6
Arabinan	1.5	1.7
Mannan	2.5	-
Acid-insoluble lignin	26.2	20.6
Acid-soluble lignin	2.3	1.7
Ash	1.8	2.4

Enzymes

A standard mixture of NS50013 and NS50010, both provided by Novozymes (Denmark), was used for the saccharification of poplar and forage sorghum WIS fractions (Negro *et al.* 2003; Manzanares *et al.* 2012). NS50013 is a cellulase preparation with some xylanase activity but practically no β-glucosidase activity; therefore, supplementation with NS50010, which mainly has β-glucosidase activity, is typically applied in a bioethanol production process. Overall cellulase activity was determined using filter paper (Whatman No. 1 filter paper strips), and β-glucosidase activity was measured using cellobiose as substrate (Ghose 1987).

One unit of enzyme activity was defined as the amount of enzyme that transforms 1 µmol of substrate per minute.

Microorganisms

Kluyveromyces marxianus CECT 10875, a thermotolerant mutant yeast strain obtained by Ballesteros *et al.* (1991), was used for the fermentation of poplar WIS fraction (Negro *et al.* 2003). *Saccharomyces cerevisiae* (Fermentis Ethanol Red, Marcq en Baroeul, France) was used for the fermentation of forage sorghum WIS fraction (Manzanares *et al.* 2012). Active cultures for inoculation were obtained in 100-mL flasks with 50 mL of growth medium containing 30 g L^{-1} glucose, 5 g L^{-1} yeast extract, 2 g L^{-1} NH_4Cl, 1 g L^{-1} KH_2PO_4, and 0.3 g L^{-1} $MgSO_4 \cdot 7H_2O$. After 16 h on a rotary shaker at 150 rpm and 42 ℃ for *K. marxianus* or 35 ℃ for *S. cerevisiae*, the pre-cultures were centrifuged at 9000 rpm for 10 min. Supernatant was discarded and cells were washed once with distilled water and then diluted to obtain the inoculum level needed.

Methods

Simultaneous Saccharification and Fermentation (SSF) Process

The SSF process with poplar WIS fraction was carried out at the optimum temperature and time conditions in 100-mL Erlenmeyer flasks containing 25 mL of sodium acetate buffer 0.1 M (pH 5.5) at solids concentration of 10% (w/w) and supplemented with the growth medium without glucose as described above (Negro *et al.* 2003). Enzyme

loadings of 15 FPU g^{-1} glucan of NS50013 and 12.6 IU g^{-1} glucan of NS50010 and 0.25 g L^{-1} (dry weight) of inoculum were also added. The SSF was run at 42 ℃ for 72 h.

The SSF process with forage sorghum WIS fraction was carried out at the optimum temperature and time conditions in 100-mL Erlenmeyer flasks containing 50 mL of sodium citrate buffer 50 mM (pH 5.5) at a solids concentration of 20% (w/w) and supplemented with the growth medium without glucose described above (Manzanares *et al.* 2012). Enzyme loadings of 20 FPU g^{-1} glucan of NS50013 and 20 IU g^{-1} glucan of NS50010 and 0.3 g L^{-1} (dry weight) of inoculum were also added. The SSF was run at 35 ℃ for 88 to 92 h.

Prior to SSF, a presaccharification step was performed by incubating the cellulolytic enzymes mixture and the pretreated biomass samples at 50 ℃ for 8 h prior to inoculation. After SSF, the lignin-enriched fermentation residues were rinsed with water and dried overnight at 60 ℃ as described by Sannigrahi and Ragauskas (2011).

Analytical Methods

The chemical compositions of raw and pretreated materials (WIS) and lignin-enriched fermentation residues were determined using the Laboratory Analytical Procedures for biomass analysis (LAP-002, LAP-003, LAP-004, LAP-017 and LAP-019) provided by the National Renewable Energies Laboratory (NREL 2007). Carbohydrate content was quantified by high-performance liquid chromatography (HPLC) in a Waters 590 chromatograph equipped with a refractive index detector (Waters, USA). A CarboSep CHO-682 carbohydrate analysis column (Transgenomic, USA), operated at 80 ℃ with ultrapure water as a mobile-phase (0.5 mL min^{-1}), was employed for the separation. Sugars concentration in SSF media was also measured by HPLC. The total nitrogen content of the lignin residues was determined by the conventional Kjeldahl method (Kjeldahl 1883).

FTIR Analysis

FTIR spectra of lignin-enriched fermentation residues were obtained using a JASCO FT/IR 460 Plus spectrometer (Jasco, Japan), equipped with an accessory single reflection diamond, operating with a resolution of 1 cm^{-1}, 400 scans, and a spectral range of 4000 to 600 cm^{-1}. FTIR bands were assigned by comparison with those reported in the literature (Faix 1991; Sun *et al.* 2002; Ibarra *et al.* 2004; She *et al.* 2010; Yuan *et al.* 2011; Sun *et al.* 2013; You *et al.* 2013). For S/G ratio estimation the intensities of the bands around 1320 cm^{-1} (syringyl units, S) and 1268 cm^{-1} (guaiacyl units, G) were estimated, after resolution enhancement (subtraction of x 1000 s derivative), moving-average smoothing (x 100) and baseline correction between valleys *ca.* 1401 and 1172 cm^{-1} (Bechtold *et al.* 1993).

NMR Analysis

NMR spectra were recorded at 25 ℃ in a Bruker AVANCE 500 MHz instrument (Bruker, USA) equipped with a z-gradient double resonance probe. Around 40 mg of lignin-enriched fermentation residues were dissolved in 0.75 mL of deuterated dimethylsulfoxide (DMSO-d_6), and the heteronuclear single quantum correlation (HSQC) experiment was recorded. The spectral widths for the HSQC were 5000 Hz and 13200 Hz for the ^1H and ^{13}C dimensions, respectively. The number of collected complex points was 2048 for ^1H-dimension with a recycle delay of 5 s. The number of transients for the HSQC spectra was 64, and 256 time increments were always recorded in ^{13}C-dimension. The *J*-coupling evolution delay was set to 3.2 ms. A squared cosine-bell apodization function was

applied in both dimensions. Prior to Fourier transform, the data matrixes were 0 up to 1024 points in the ^{13}C-dimension. Residual DMSO (from DMSO-d$_6$) was used as reference for chemical shifts. Two-dimensional NMR cross-signals were assigned by comparison with those reported in the literature (Ralph *et al.* 1999; Ralph *et al.* 2004; Ibarra *et al.* 2007a; del Río *et al.* 2008; Ralph *et al.* 2010; Samuel *et al.* 2011a,b; Yuan *et al.* 2011; del Río *et al.* 2012; Sun *et al.* 2013; You *et al.* 2013).

Semi-quantitative analysis of the HSQC cross-signal intensities was performed (Martínez *et al.* 2008; Sun *et al.* 2013). Volume integration of the cross-signals was performed separately for the different regions of the HSQC spectra, which contain signals that correspond to chemically analogous carbon-proton pairs. For these signals, the $^1J_{CH}$ coupling value is relatively similar and suitable for semi-quantitative estimation of the different C–H correlations. In the aliphatic oxygenated region, inter-unit linkages were estimated from C$_\alpha$–H$_\alpha$ correlations to avoid possible interference from homonuclear ^{1}H–^{1}H couplings, and the relative abundance of side chains involved in inter-unit linkages and terminal structures was calculated (with respect to total side chains). In the aromatic region, C$_2$–H$_2$ correlations from H, G and S lignin units and from *p*-hydroxybenzoate, *p*-coumarate, and ferulate were used to estimate their relative abundances.

RESULTS AND DISCUSSION

Pretreatment and SSF Process: Chemical Composition

Steam explosion was used as the pretreatment for poplar and forage sorghum in an effort to improve the enzymatic hydrolysis and increase the fermentable sugars yields (Alvira *et al.* 2010). Under high temperature and pressures water causes an auto-catalyzed cleavage of glycosidic bonds in hemicelluloses and lignin-hemicelluloses linkages. This, along with the production of acetic acid from acetyl groups, facilitates the removal of hemicelluloses from the plant cell wall, making cellulose more accessible to enzymes (Alvira *et al.* 2010). These effects could be seen in poplar and forage sorghum after being subjected to steam explosion pretreatment (Table 2). Compared to the cellulose content of both untreated materials (39.5%, poplar; 35.4%, forage sorghum), pretreatment increased the cellulose proportion in their respective WIS fractions (57.2%, poplar; 57.3% forage sorghum) due to the extensive removal of hemicelluloses content (from 22.0% of untreated poplar to 3.3% of WIS fraction; and from 22.8% of untreated forage sorghum to 3.8% of WIS fraction). It was also clear that the relative lignin content increased after pretreatment (from 26.2% of untreated poplar to 35.3% of WIS fraction; and from 20.6% of untreated forage sorghum to 33.8% of WIS fraction). This increase was attributed, in part, to the removal of hemicelluloses and also to the accumulation of non-lignin based material formed by acid catalysed condensation of polysaccharides during pretreatment (Li *et al.* 2007).

SSF process was carried out with the WIS fractions from poplar and forage sorghum at optimum conditions based on enzymatic hydrolysis yields (Negro *et al.* 2003; Manzanares *et al.* 2012). As expected, the SSF process concentrated the lignin in both fermentation residues, showing lignin content increments of 92% and 130% for poplar and forage sorghum, respectively (Table 2). Nevertheless, certain sugars still remained in both residues, being lower in forage sorghum (29.6%, poplar; 11.7%, forage sorghum) according with its higher enzymatic hydrolysis yield (60%, poplar; 89%, forage sorghum). The higher severity factor Log(Ro) of steam explosion pretreatment on forage sorghum

(4.37), compared to poplar (3.83), could be one of the reasons for the major enzymatic hydrolysis efficiency of the pretreated sorghum and, consequently, the lower remaining sugars content in the fermentation residue.

Together with sugars, both fermentation residues also showed a high nitrogen content (0.6% poplar; 2%, forage sorghum), which indicates the presence of protein impurities from hydrolytic enzymes used for saccharification.

Table 2. Chemical Composition of WIS Fractions and Lignin-enriched Fermentation Residues from Fast-growing Poplar and Forage Sorghum

WIS			Fermentation Residue		
Composition (% dry weight)	Poplar	Forage Sorghum	Composition (% dry weight)	Poplar	Forage Sorghum
Cellulose	57.2	57.3	Glucose	27.0	9.7
Hemicelluloses	3.3	3.8	Xylose	1.3	1.1
Lignin	35.3	33.8	Galactose	0.1	0.1
			Arabinose	0.0	0.0
			Mannose	1.2	0.8
			Lignin	67.9	77.7
SSF yields of 60% and 85% of theoretical for poplar and forage sorghum, respectively					

FTIR Spectral Analysis

Figure 1 shows the FTIR spectra of the lignin-enriched fermentation residues resulting from the SSF process of poplar and forage sorghum WIS fractions, respectively. According to the chemical composition reported above, these spectra were clearly dominated by lignin bands. The wide band observed around 3334 cm^{-1} represented the O–H stretching vibration in aromatic and aliphatic structure, and the bands at 2926 and 2838 cm^{-1} were due to a C–H vibration sketch in the CH$_2$ and CH$_3$ groups, respectively. The bands at 1710 cm^{-1} (shoulder) and 1657-1647 cm^{-1} represented the C=O bonds in non-conjugated and conjugated ketones, respectively. Nevertheless, the latter also is associated with carbonyl stretching in amide bonds from protein from the residual enzymes used for saccharification (Ibarra *et al.* 2004). The bands at 1591, 1507 and 1422 cm^{-1} were attributed to aromatic skeleton vibrations, whereas a band at 1455 cm^{-1} that corresponded to the C–H asymmetric vibrations and deformations (asymmetric in methyl and methylene) was also observed. The poplar spectrum showed a higher intensity of lignin bands assigned to syringyl units, at 1320 cm^{-1} (aromatic ring breathing, S and G$_{condensed}$ units) and 833 cm^{-1} (out-of-plane C–H bending in position 2 and 6), than that of guaiacyl units, at 1268 cm^{-1} (aromatic ring breathing) and 913 cm^{-1} (out-of-plane aromatic C–H bending) (Fig. 1a). By contrast, forage sorghum spectrum showed the features of HGS type lignin, with the typical bands at 1163 and 833 cm^{-1}, the latter corresponding to C–H out-of-plane in all positions of *p*-hydroxyphenyl units (Fig. 1b). These intensity differences were reflected in the S/G values, revealing the presence of a S-type lignin in poplar (S/G ratio of 1) and G-type lignin in forage sorghum (low S/G ratio of 0.2). Finally, the band at 1163 cm^{-1} also corresponds to antisymmetric C–O stretching of ester groups (Sun *et al.* 2002), indicating the presence of ester-linked hydroxycinnamic acids (*p*-coumaric, PCA; and ferulic acid, FA, showed in Fig. 3) in forage sorghum (Fig. 1b).

The remaining sugars content of the lignin residues was also visible in both spectra, with a polysaccharide region at 1110 to 1030 cm^{-1} dominated by ring vibrations overlapped with stretching vibration of C–OH side groups and the C–O–C glycosidic bond vibration.

a)

b)
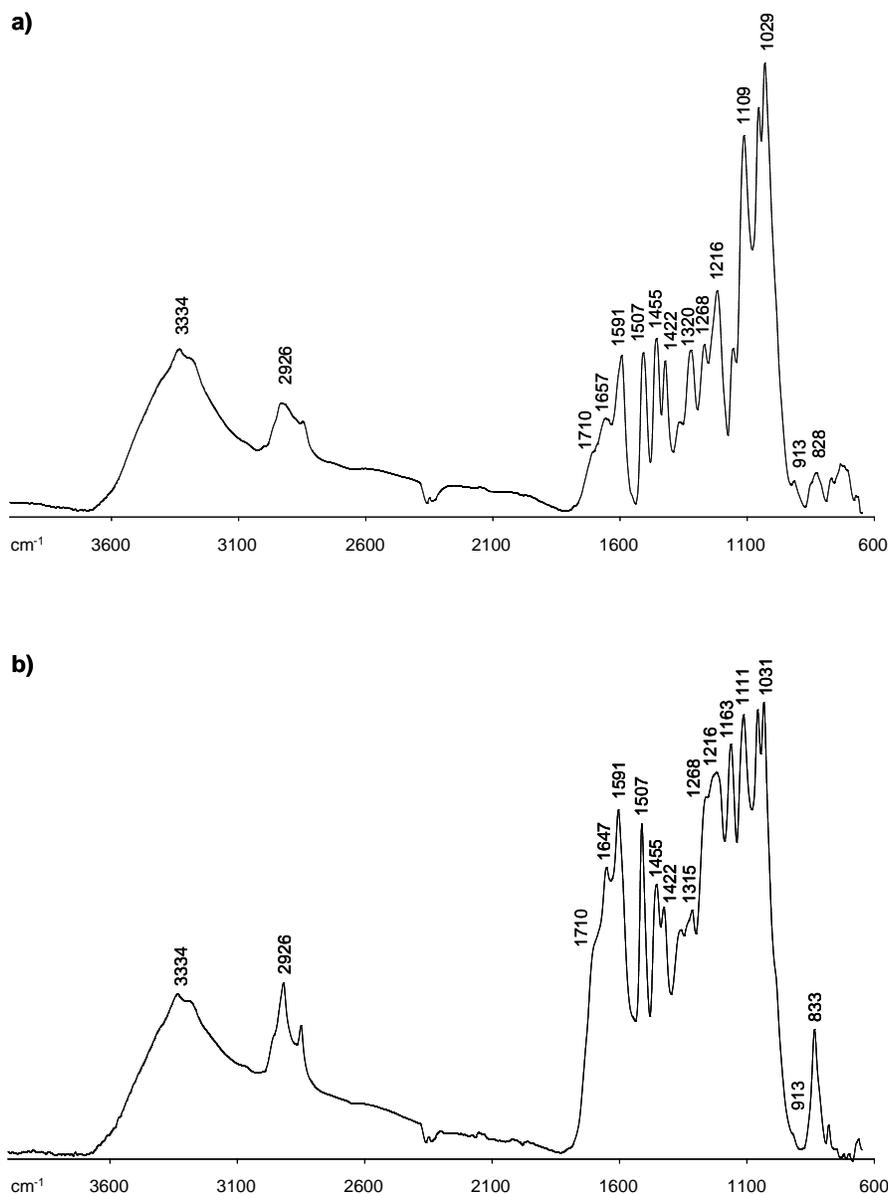

Fig. 1. FTIR spectra, 4000 to 600 cm^{-1} region, of the lignin-enriched fermentation residues from fast-growing poplar a) and forage sorghum b) WIS fractions

2D-NMR Spectral Analysis: HSQC Spectra

HSQC NMR spectra of the lignin-enriched fermentation residues also showed the predominance of lignin signals together with the remaining sugars and some protein impurities (Fig. 2). The main structural characteristics of both lignins, including different units linked by ether and C–C bonds, and carbohydrates are represented in Fig. 3. Their corresponding cross-signals are listed in Table 3.
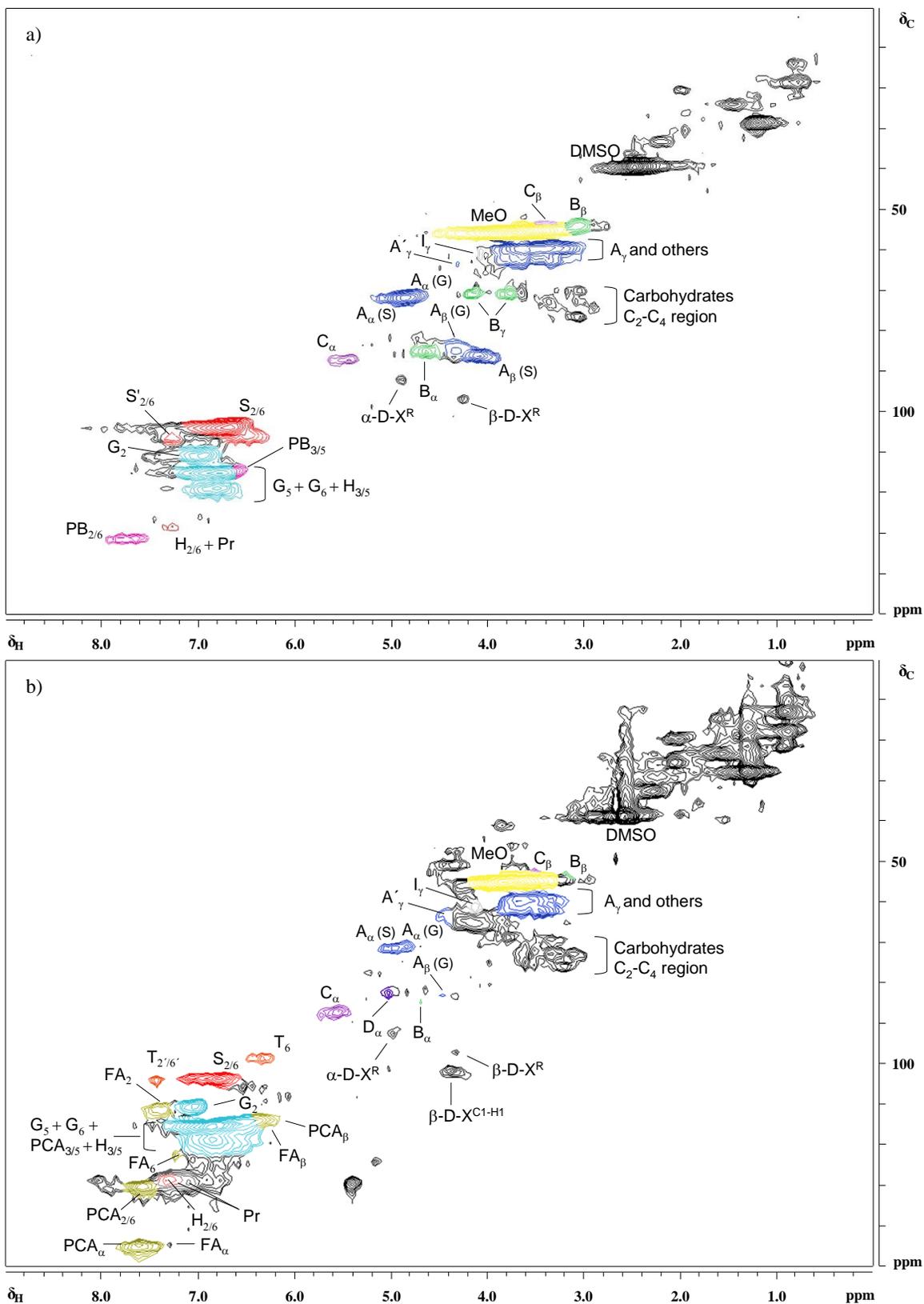
Fig. 2. HSQC 2D-NMR spectra, δC/δH 0–150/0–9 ppm region, of the fermentation residues from fast-growing poplar a) and forage sorghum b) WIS fractions. The aliphatic, oxygenated aliphatic, and aromatic regions are observed. Cross-signals of the residual DMSO and protein (Pr) impurities are indicated.
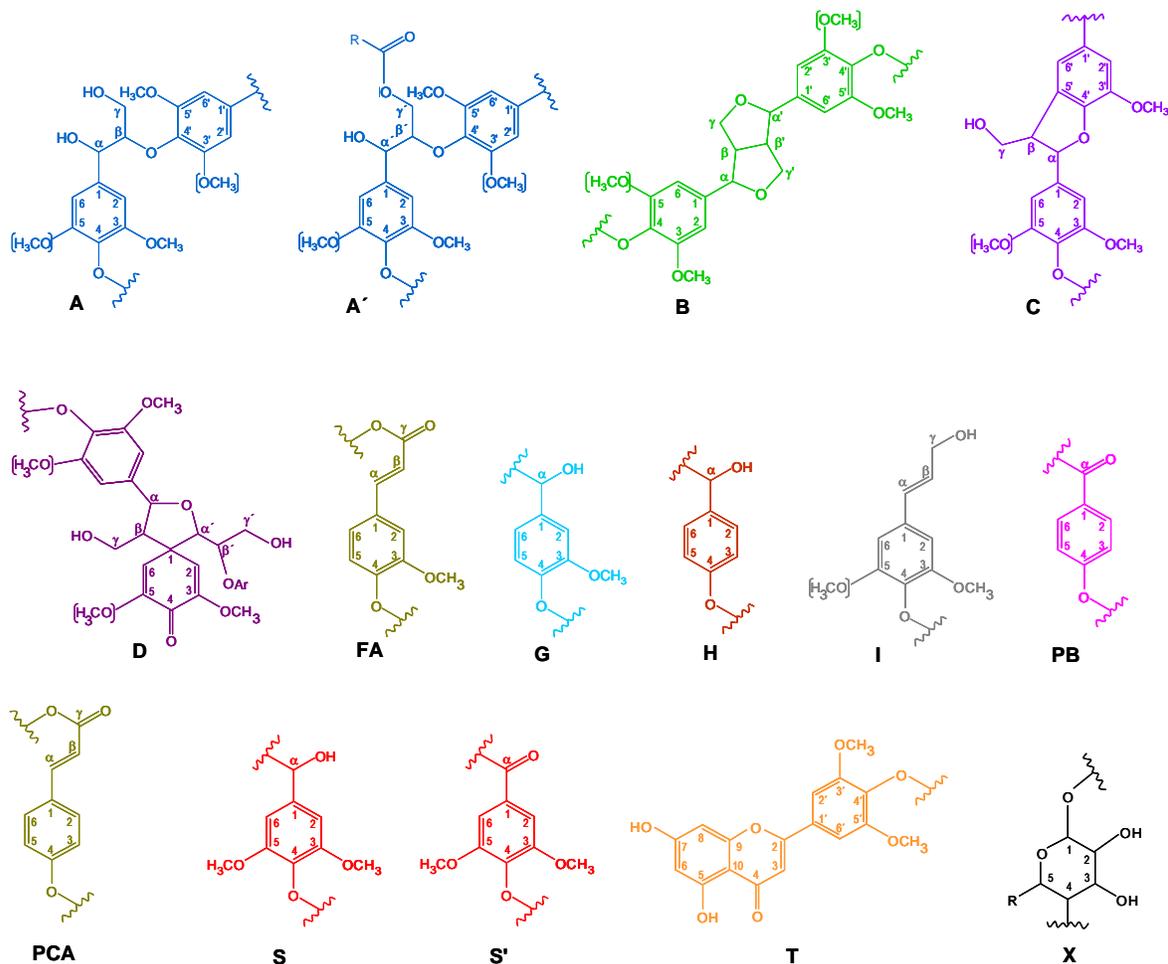
Fig. 3. Main lignin and carbohydrate structures identified in the fermentation residues from fast-growing poplar and forage sorghum WIS fractions: **A**, β-O-4´; **A´**, β-O-4´ with γ-OH acylated (R, p–hydroxybenzoylated in poplar or p-coumaroyl in forage sorghum); **B**, resinols with β-β´, α-O-γ´, and γ-O-α´ linkages; **C**, phenylcoumarans with α-O-4´ and β-5´ linkages; **D**, spirodienones with β-1´, α-O-4´ linkages; **FA**, ferulic acid; **G**, guaiacyl unit; **H**, p-hydroxyphenyl unit; **I**, p-hydroxycinnamyl alcohol terminal unit; **PB**, p-hydroxybenzoate; **PCA**, p-coumaric acid; **S**, syringyl unit; **S´**, oxidized syringyl units with a Cα ketone; **T**, tricin end unit; **X**, xylopyranose (R, OH).

The HSQC spectra showed three regions corresponding to aliphatic, oxygenated aliphatic, and aromatic $^{13}C-^{1}H$ correlations. No cross-signals were observed in the δ_C 150 to 205 ppm region (that is not shown in Fig. 2). The non-oxygenated aliphatic region (around δ_C/δ_H 0–50/0–4.5 ppm) showed a wide variety of saturated aliphatic moieties with relatively high intensities, especially in the forage sorghum spectrum. Some strong signals in this area (δ_H 0.8 and δ_H 1.2–1.3) correspond to extractives (Balakshin *et al.* 2003; Martín-Sampedro *et al.* 2011). All other chemical shifts of about δ_H 1.5 to 2.5 correspond to aliphatic groups neighboring alkene and oxygen-containing groups, such as alcohol, carbonyl, and ether, which may be a consequence of lignin degradation products (Martín-Sampedro *et al.* 2011; Fernández-Costas *et al.* 2014).

Table 3. Assignment of Main Lignin and Sugars ^{13}C–^{1}H Cross-signals in the HSQC Spectra of Fermentation Residues from Fast-growing Poplar and Forage Sorghum WIS Fractions

δ_C/δ_H (ppm)	Assignment
53.7/3.42	C_β–H_β in phenylcoumaran substructures (**C**)
54.1/3.04	C_β–H_β in resinol substructures (**B**)
55.6/3.7	C-H in methoxyls (**MeO**)
60.1/3.4–3.7	C_γ–H_γ in β-O-4´ substructures (**A**)
61.4/4.1	C_γ–H_γ in cinnamyl alcohol end groups (**I**)
63.5/4.37	C_γ–H_γ in β-O-4´ substructures (**A´**)
71.0/4.75	C_α–H_α in β-O-4´ linked to a **G** type unit (**A**)
70.9/3.77–4.14	C_γ–H_γ in resinol substructures (**B**)
71.9/4.83	C_α–H_α in β-O-4´ linked to a **S** type unit (**A**)
82.5/4.9	C_α–H_α in spirodienone substructures (**D**)
84.1/4.3	C_β–H_β in β-O-4´ linked to a **G** type unit (**A**)
85.4/4.64	C_α–H_α in resinol substructures (**B**)
86.5/4.2	C_β–H_β in β-O-4´ linked to a **S** type unit (**A**)
87.4/5.4	C_α–H_α in phenylcoumaran substructures (**C**)
92.3/4.88	(1→4)-linked α-D-xylopyranosyl units (**α-D-X^R**)
97.0/4.2	(1→4)-linked β-D-xylopyranosyl units (**β-D-X^R**)
98.8/6.20	C_6–H_6 in tricin (**T**)
102.5/4.37	(1→4)-linked β-D-xylopyranosyl units (**β-D-X^{C1-H1}**)
104.7/6.7	$C_{2,6}$–$H_{2,6}$ in S units (**S**)
104.0/7.31	$C_{2'}$–$H_{2'}$ and $C_{6'}$–$H_{6'}$ in tricin (**T**)
106.7/7.2	$C_{2,6}$–$H_{2,6}$ in oxidized (C_α=O) S units (**S´**)
111.0/6.99	C_2–H_2 in G units (**G**)
111.0/7.32	C_2–H_2 in ferulate (**FA**)
113.5/6.27	C_β–H_β in p-coumarate (**PCA**) and ferulate (**FA**)
114.3/6.61	$C_{3,5}$–$H_{3,5}$ in p-hydroxybenzoate (**PB**)
115.2/6.7-6.9	C_5–H_5 in G units (**G**)
115.2/6.74	$C_{3,5}$–$H_{3,5}$ in p-hydroxyphenyl (**H**)
115.4/6.79	C_3–H_3 and C_5–H_5 in p-coumarate (**PCA**)
119.6/6.81	C_6–H_6 in G units (**G**)
123.2/7.15	C_6–H_6 in ferulate (**FA**)
128/7.17	$C_{2,6}$–$H_{2,6}$ in p-hydroxyphenyl (**H**)
129.8/7.51	C_2–H_2 and C_6–H_6 in p-coumarate (**PCA**)
131.4/7.78	$C_{2,6}$–$H_{2,6}$ in p-hydroxybenzoate (**PB**)
143.8/7.49	C_α–H_α in p-coumarate (**PCA**) and ferulate (**FA**)

In the oxygenated aliphatic region (around δ_C/δ_H 50–95/2.6–5.6 ppm), cross-signals of methoxyl groups (–OCH_3, δ_C/δ_H 55.6/3.7 ppm) and the different inter-unit linkages of poplar and forage sorghum lignins were detected (Fig. 2). The poplar spectrum showed prominent signals corresponding to β-O-4´ substructures (A). The C_α–H_α correlations in β-O-4´ substructures were observed in overlapping signals at δ_C/δ_H 71.0/4.75 and 71.9/4.83 ppm for structures linked to G or S lignin units. Likewise, the C_β–H_β correlations were found at δ_C/δ_H 84.1/4.3 ppm for β-O-4´ G units and at δ_C/δ_H 86.5/4.2 ppm for β-O-4´ S units. The C_γ–H_γ correlations in β-O-4´ substructures were observed at δ_C/δ_H 60.1/3.4 and 3.7 ppm, partially overlapped with other signals. This set of signals assigned to β-O-4´ substructures was also detected in the forage sorghum spectrum, although in lower intensities. Strong signals for resinol (β-β´) substructures (B) were also detected in the spectrum of poplar, with their C_α–H_α, C_β–H_β, and the double C_γ–H_γ correlations at δ_C/δ_H

85.4/4.64, 54.1/3.04 and 70.9/3.77 and 4.14 ppm (*i.e.*, the two diastereotopic protons attached to the γ carbon). By contrast, the signals for resinol substructures showed very low proportions in forage sorghum spectrum. Phenylcoumaran (β-5´) substructures (C) were clearly found in both spectra, the signals for their C_α–H_α and C_β–H_β correlations being observed at δ_C/δ_H 87.4/5.4 and 53.7/3.42 ppm. A small signal corresponding to spirodienone substructures (D) was also observed in the forage sorghum spectrum, its C_α–H_α correlation being at δ_C/δ_H 82.54/4.9 ppm. Finally, other signals detected in the oxygenated aliphatic region of both spectra corresponded to the C_γ–H_γ correlations of cinnamyl alcohol end-groups (I) at δ_C/δ_H 61.4/4.1 ppm.

The remaining sugars in both lignin residues were displayed by a set of unidentified cross-signals in the δ_C/δ_H 67–75/3.0–3.8 ppm region that could correspond to hexose units in carbohydrates. In addition, the reducing ends of (1→4) α-D-xylopyranosyl units (α-D-X^R) and (1→4) β-D-xylopyranosyl units (β-D-X^R) were presented in both spectra at δ_C/δ_H 92.3/4.88 and 97.0/4.2 ppm, respectively. On the other hand, the C_1–H_1 cross-signal of (1→4) β-D-xylopyranosyl units (β-D-X^{C1-H1}) at δ_C/δ_H 102.5/4.37 ppm was only observed in forage sorghum spectrum.

The main cross-signals in the aromatic region (around δ_C/δ_H 95–150/5.6–9.0 ppm) of both spectra (Fig. 2) corresponded to the aromatic rings of the different S and G lignin units. The S lignin units showed a prominent signal for the $C_{2,6}$–$H_{2,6}$ correlation at δ_C/δ_H 104.7/6.7 ppm. In addition, signals corresponding to $C_{2,6}$–$H_{2,6}$ correlations at δ_C/δ_H 106.7/7.2 ppm in C_α oxidized S units were only present in the poplar spectrum. It has been identified as C_α ketone by HMBC (heteronuclear multiple bond correlation) 2D-NMR experiments (Ibarra *et al.* 2007b). The G lignin units showed different correlations for C_2–H_2 (δ_C/δ_H 111.0/6.99 ppm) and C_5–H_5/C_6–H_6 (δ_C/δ_H 115.2/6.7 and 6.9 ppm, and δ_C/δ_H 119.6/6.81 ppm). Signals corresponding to $C_{3,5}$–$H_{3,5}$ and $C_{2,6}$–$H_{2,6}$ correlations in H lignin units were also observed at δ_C/δ_H 115.2/6.74 and δ_C/δ_H 128/7.17 ppm, respectively, being specially intense in forage sorghum spectrum. Nevertheless, the signal corresponding to $C_{2,6}$–$H_{2,6}$ was partially overlapped by the cross-signals at δ_C/δ_H 128.5/7.24 and 130.1/7.03 from protein contamination (Chen *et al.* 2003), hindering an appropriate H lignin analysis.

Prominent signals for the $C_{2,6}$–$H_{2,6}$ and $C_{3,5}$–$H_{3,5}$ correlations of *p*-hydroxybenzoate substructures (PB) were found in poplar at δ_C/δ_H 131.4/7.78 and δ_C/δ_H 114.3/6.61 ppm, respectively (Fig. 2a). The presence of *p*-hydroxybenzoates has already been reported in many plants, including poplar, mostly acylating the γ–OH of the lignin side chain (Meyermans *et al.* 2000; Moreel *et al.* 2004; Ralph *et al.* 2010; del Río *et al.* 2012). Moreover, Morreel *et al.* (2004) had found that only S units are γ–*p*–hydroxybenzoylated in poplar lignin. In this sense, the oxygenated aliphatic region of poplar spectrum showed a very weak signal at δ_C/δ_H 63.5/4.37 ppm corresponding to the C_γ–H_γ correlations of γ-acylated β-*O*-4´ substructures (A´) with *p*-hydroxybenzoate. Regarding the forage sorghum spectrum, prominent signals corresponding to *p*-coumarate (PCA) and ferulate (FA) substructures were seen (Fig. 2b), as is typical in spectra from this and other grasses (Ralph *et al.* 2010; Sun *et al.* 2013; You *et al.* 2013); this was in agreement with the FTIR analysis. Cross-signals corresponding to the $C_{2,6}$−$H_{2,6}$ at δ_C/δ_H 129.8/7.51 ppm and $C_{3,5}$−$H_{3,5}$ at δ_C/δ_H 115.4/6.79 ppm correlations of the aromatic ring and signals for the correlations of the unsaturated C_α–H_α at δ_C/δ_H 143.8/7.49 ppm and C_β–H_β at δ_C/δ_H 113.5/6.27 ppm of the *p*-coumarates were observed. Signals corresponding to the C_2−H_2 and C_6–H_6 correlations of ferulate substructures were also observed at δ_C/δ_H 111.0/7.32 and 123.3/7.15 ppm, respectively. The correlations corresponding to the unsaturated C_α–H_α and C_β–H_β

overlapped with those of the *p*-coumarates. Previous studies have indicated that *p*-coumarates in sorghum are esterified to the lignin side chain (Sun *et al.* 2002; She *et al.* 2010), probably acylating the γ–OH of the lignin side chain as established for other grasses (del Río *et al.* 2008; Ralph *et al.* 2010). As indicated for poplar, the oxygenated aliphatic region of forage sorghum spectrum also showed a very weak signal at δ_C/δ_H 63.5/4.37 ppm corresponding to the C_γ–H_γ correlations of γ-acylated β-O-4´ substructures (A´) with *p*-coumarates. Ferulates, on the other hand, are mostly linked to lignin by ether bonds (Sun *et al.* 2002; She *et al.* 2010), mainly at the α- and β-carbons contributing to lignin–carbohydrate bridges (Ralph *et al.* 2004). Finally, some cross-signals of tricin (T, 5,7,4´-trihydroxy-3´-5´-dimethoxyflavone) arose in the spectra of forage sorghum (Fig. 2b). The tricin signals corresponded to aromatic C_6−H_6 and $C_{2´,6´}$−$H_{2´,6}$ were detected at δ_C/δ_H 98.8/6.2 and 104.0/7.31 ppm, respectively. As is well known, tricin is widely distributed in grasses, including wheat, rice, barley, sorghum, and maize (Zhou and Ibrahim 2010). A tricin skeleton can be linked to a phenylpropanoid moiety through a β-O-4´ bond, which may happen in the lignification of plants, acting as lignin monomers (del Río *et al.* 2012).

2D-NMR Spectral Analysis: Semiquantitative HSQC Spectra

The relative abundances of the main inter-unit linkages and end-groups, as well as the percentage of γ-acylation, the molar abundances of the different lignin units (H, G, and S), *p*-hydroxybenzoates, *p*-coumarates and ferulates, and the molar S/G ratios of the lignins in poplar and forage sorghum fermentation residues, estimated from volume integration of contours in HSQC spectra (Martínez *et al.* 2008; Sun *et al.* 2013), are shown in Table 4.

It is well documented that the degradation of β-O-4´ structures is the main reaction in lignin in steam explosion pretreatment (Li *et al.* 2007; Alvira *et al.* 2010; Samuel *et al.* 2011a; Yelle *et al.* 2013). During steam explosion, the steam cleaves labile xylans acetyls (2-*O*-Ac-β-D-Xyl*p* and 3-*O*-Ac-β-D-Xyl*p*) and 4-*O*-methyl glucuronic acid (4-*O*-MeGlcA), thus releasing acetic acid and uronic acid. Then, these organic acids released lead to acid catalyzed hydrolysis (acidolysis) of glycosidic bonds in hemicelluloses and of β-O-4´ linkages in lignin (Li *et al.* 2007; Alvira *et al.* 2010). In spite of this fact, the semiquantitative HSQC spectrum results of poplar residual lignin demonstrated an important content of β-O-4´ aryl ether linkages (66%). Furthermore, minor amounts of β-$\beta´$ resinols (21%), β-5´ phenylcoumarans (13%), and terminal structures such as cinnamyl alcohol end-groups (3%) were also determined. About them, the literature has reported contradictory results during the bioethanol production process. Yelle *et al.* (2013) described that resinols and phenylcoumarans withstand the steam explosion of wheat straw, although with substantial removal of cinnamyl alcohol end-groups. By contrast, Rahikainen *et al.* (2013) observed an increment in the level of β-5´ inter-unit linkages after the steam explosion treatment of wheat straw due to a possible rearrangement between inter-unit linkages. Finally, other studies reflected the degradation of these substructures during the steam pretreatment of materials such as poplar wood and switchgrass (Samuel *et al.* 2011a,b).

As for other hardwoods (Ralph *et al.* 1999; Ibarra *et al.* 2007a; Samuel *et al.* 2011b), the poplar lignin aromatic region displayed a predominance of S lignin units (67%) followed by G (32%) and H units (traces). Nevertheless, the S/G ratio calculated by 2D-NMR (S/G ratio of 2.1) was higher than the ratio calculated previously by FTIR (S/G ratio of 1.0). In addition, the abundance of *p*-hydroxybenzoate was 5%. Different changes in the lignin aromatic region during the bioethanol production have been also documented in the

literature. Samuel *et al.* (2011a,b) reported a noticeable decrease in the relative intensities of the S, G, and H lignin units during the steam pretreatment of poplar and switchgrass. In addition, the content of *p*-hydroxybenzoate, in poplar, and *p*-hydroxycinnamates, in switchgrass, was reduced in a significant degree. By contrast, the poplar lignin aromatic region studied herein still displayed significant contour intensities of the S, G, H, and *p*-hydroxybenzoate resonances. In the same way, Yelle *et al.* (2013) did not observe changes in the syringyl/guaiacyl/*p*-hydroxyphenyl distribution and *p*-hydroxycinnamates of steam-exploded wheat straw residual lignin. This fact, together with the important content of lignin side-chains described above, could indicate an insignificant degree of degradation of poplar lignin during the steam explosion pretreatment and the subsequent SSF process.

Table 4. Structural Characteristics of Lignin (Main Inter-unit Linkages, End-Groups, γ-Acylation, Aromatic Units, and S/G Ratio, *p*-Hydroxycinnamate Content, and *p*-Coumarate/Ferulate Ratio) from Integration of ^{13}C–^{1}H Correlation Peaks in the HSQC Spectra of the Fermentation Residues from Fast-growing Poplar and Forage Sorghum WIS Fractions

	Poplar	Forage Sorghum
Lignin inter-unit linkages		
β-O-4´ (**A/A´**)	66	50
resinols (**B**)	21	5
phenylcoumarans (**C**)	13	37
spirodienones (**D**)	-	8
Lignin end-groups		
cinamyl alcohol end-groups (**I**)	3	4
Lignin side-chain γ-acylation	traces	4
Lignin aromatic units		
H	traces	4
G	32	49
S	67	47
S/G ratio	2.1	0.9
p-hydroxybenzoate (**PB**)	5	-
p-hydroxycinnamates		
p-coumarates (**PCA**)	-	35
ferulates (**FA**)	-	17
PCA/**FA** ratio	-	2

Forage sorghum residual lignin also displayed a predominance of *β-O*-4´ aryl ether linkages (50%), followed by *β*-5´ phenylcoumarans (37%), spirodienones (8%), and *β-β´* resinols (5%). Compared to poplar, forage sorghum lignin showed lower intensities of lignin side chain signals, especially *β-O*-4´ and resinol substructures (Fig. 2). This could indicate a greater lignin degradation as a consequence of the higher pretreatment conditions used for forage sorghum biomass (220 ºC, 7 min; equivalent to a severity factor $Log(R_0)$ of 4.37) compared to poplar (210 ºC, 4 min; equivalent to a severity factor $Log(R_0)$ of 3.83). In addition, the higher proportion of H lignin units (4%) in forage sorghum, a characteristic of grasses (Ralph and Landucci 2010; Sun *et al.* 2013; You *et al.* 2013), allows a higher accessibility of hydrolytic agents as H units are essentially all terminal (Yelle *et al.* 2013).

Finally, the S/G ratio of the forage sorghum residual lignin was significantly lower (0.9) than that of poplar residual lignin, higher compared to that estimated above by FTIR (0.2), with a higher proportion of H units (4%) and a *p*-hydroxycinnamates ratio of 2.0.

Potential Industrial Application of Lignins with Respect to their Structural Characteristics

In spite of depolymerization reactions described in the literature during the bioethanol production process (Li *et al.* 2007; Alvira *et al.* 2010; Samuel *et al.* 2011a; Yelle *et al.* 2013), the residual lignins from bioethanol production of fast-growing poplar and forage sorghum studied herein showed clearly a higher abundance of native *β-O-4´* aryl ether linkages compared to the traditional industrial lignins such as kraft lignin and soda-AQ lignin (Prinsen *et al.* 2013; Fernández-Costas *et al.* 2014). This high content of alkyl-aryl ether linkages would result in a high molecular mass lignin, which could be an advantage in lignin based dispersants providing better sorption properties, and be beneficial in respect of mechanical properties of lignin based composites (Vishtal and Kraslawski, 2011). In addition to this use of lignin as macromolecule in materials such as dispersants and composites, lignin is an important source for aromatic chemicals (Ragauskas *et al.* 2010). Different approaches have been reported for its conversion into low molecular weight chemicals, including thermochemical treatments and catalytic technology (Ragauskas *et al.* 2010; Vishtal and Kraslawski 2011). Lignin with a predominance of syringyl units is more favorable for thermal or catalytic depolymerization, because methoxy substituents in *ortho* positions of the aromatic ring minimize the presence of unreactive carbon-carbon linkages (Ragauskas *et al.* 2010). Thus, the residual lignin for poplar, with a higher S lignin content compared to forage sorghum, would be more reactive to thermal and chemical fragmentation. Nevertheless, the contamination by sugars and protein impurities determined in these lignins may significantly affect their applicability, that is, lignin as macromolecule and lignin-aromatic chemicals. To address such issues, different purification methods based on acid/base extraction or enzymatic treatments have been proposed (Vishtal and Kraslawski, 2011).

CONCLUSIONS

1. The fermentation residues from the bioethanol production process, including steam-explosion, saccharification, and fermentation, of fast-growing poplar and forage sorghum were characterized.

2. The chemical compositions and FTIR and 2D-NMR spectroscopy analyses confirmed the high lignin content, together with some sugar and protein impurities, of both fermentation residues.

3. A strong predominance of *β-O-4´* linkages, followed by resinols and phenylcoumarans, were found in both lignins. Poplar showed a typical GS lignin with a predominance of S over G units and the presence of some amount of *p*-hydroxybenzoate, whereas a typical HGS lignin was observed for forage sorghum with a lower S/G ratio and higher proportions of H lignin units and *p*-hydroxycinnamates.

4. These structural characteristics determine the use of these lignins in respect to their valorization. Then, the high content of native aryl ether linkages in both residual lignins

would result in high molecular mass lignins. Based of this, poplar and forage sorghum residual could be beneficial as macromolecules for dispersants and composites. In addition, low molecular weight chemicals could also be produced from residual lignins, being poplar lignin potentially more reactive to depolymerization reactions.

ACKNOWLEDGMENTS

REFERENCES CITED

Alvira, P., Tomás-Pejó, E., Ballesteros, M., and Negro, M. J. (2010). "Pretreatment technologies for an efficient bioethanol production process based on enzymatic hydrolysis: a review," *Bioresour. Technol.* 101, 4851-4861. DOI: 10.1016/j.biortech.2009.11.093

Balakshin, M. Y., Capanema, E. A., Chen, D., and Gracz, H. S. (2003). "Elucidation of the structures of residual and dissolved pine kraft lignins using an HMQC NMR technique," *J. Agric. Food Chem.* 51(21), 6116-6127. DOI: 10.1021/jf034372d

Ballesteros, I., Ballesteros, M., Cabañas, A., Carrasco, J., Martín, C., Negro, M. J., Sáez, F., and Sáez, R. (1991). "Selection of thermotolerant yeasts for simultaneous saccharification and fermentation (SSF) of cellulose to ethanol," *Appl. Biochem. Biotechnol.* 28, 307-315. DOI: 10.1007/BF02922610

Ballesteros, M., Oliva, J. M., Negro, M. J., Manzanares, P., and Ballesteros, I. (2004). "Ethanol from lignocellulosic materials by a simultaneous saccharification and fermentation process (SFS) with *Kluyveromyces marxianus* CECT 10875," *Process Biochem.* 39, 1843-1848. DOI: 10.1016/j.procbio.2003.09.011

Bechtold, R., González, A. E., Almendros, G., Martínez, M. J., and Martínez, A. T. (1993). "Lignin alteration by *Ganoderma australe* and other white-rot fungi after solid-state fermentation of beech wood," *Holzforschung* 47, 91-96. DOI: 10.1515/hfsg.1993.47.2.91

Chen, C.-L., Capanema, E. A., and Gracz, H. S. (2003). "Comparative studies on the delignification of pine kraft-anthraquinone pulp with hydrogen peroxide by binucleus Mn(IV) complex catalysis," *J. Agric. Food. Chem.* 51, 6223-6232. DOI: 10.1021/jf034507f

Christersson, L. (2008). "Poplar plantations for paper and energy in the south of Sweden," *Biomass Bioener.* 32, 997-1000. DOI: 10.1016/j.biombioe.2007.12.018

del Río, J. C., Rencoret, J., Marques, G., Gutiérrez, A., Ibarra, D., Santos, J. I., Jiménez-Barbero, J., Zhang, L., and Martínez, A. T. (2008). "Highly acylated (acylated and/or p-coumaroylated) native lignins from diverse herbaceous plants," *J. Agric. Food Chem.* 56, 9525-9534. DOI: 10.1021/jf800806h

del Río, J. C., Rencoret, J., Prinsen, P., Martínez, A. T., Ralph, J., and Gutiérrez, A. (2012). "Structural characterization of wheat straw lignin as revealed by analytical

pirólisis, 2D-NMR, and reductive cleavage methods," *J. Agric. Food Chem.* 60, 3619-3634. DOI: 10.1021/jf301002n

Faix, O. (1991). "Classification of lignins from different botanical origins by FTIR spectroscopy," *Holzforschung.* 45, 21-27. DOI: 10.1515/hfsg.1991.45.s1.21

Fernández-Costas, C., Gouveia, S., Sanromán, M. A., and Moldes, D. (2014). "Structural characterization of kraft lignins from different spent cooking liquors by 1D and 2D nuclear magnetic resonance spectroscopy," *Biomass Bioenerg.* 63, 156-166. DOI: 10.1016/j.biombioe.2014.02.020

Ghose, T. K. (1987). "Measurement of cellulase activity," *Pure Appl. Chem.* 59, 257-268. DOI: 10.1351/pac198759020257

Ibarra, D., del Río, J. C., Gutiérrez, A., Rodríguez, I. M., Romero, J., Martínez, M. J., and Martínez, A. T. (2004). "Isolation of high-purity residual lignins from eucalypt paper pulps by cellulase and proteinase treatments followed by solvent extraction," *Enzyme Microb. Technol.* 35, 173-181. DOI: 10.1016/j.enzmictec.2004.04.002

Ibarra, D., Chávez, M. I., Rencoret, J., del Río, J. C., Gutiérrez, A., Romero, J., Camarero, S., Martínez, M. J., Jiménez-Barbero, J., and Martínez, A. T. (2007a). "Lignin modification during *Eucalyptus globulus* kraft pulping followed by totally chlorine free bleaching: A two-dimensional nuclear magnetic resonance, Fourier transform infrared, and pyrolysis-gas chromatography/mass spectrometry study," *J. Agric. Food Chem.* 55, 3477-3490. DOI: 10.1021/jf063728t

Ibarra, D., Chávez, M. I., Rencoret, J., del Río, J. C., Gutiérrez, A., Romero, J., Camarero, S., Martínez, M. J., Jiménez-Barbero, J., and Martínez, A. T. (2007b). "Structural modification of eucalypt pulp lignin in a totally chlorine-free bleaching sequence including a laccase-mediator stage," *Holzforschung* 61, 634-646. DOI: 10.1515/HF.2007.096

Kjeldahl, J. (1883). "A new method for the determination of nitrogen in organic matter," *Z. Anal. Chem.* 22, 366-382.

Li, J., Henriksson, G., and Gellersted, G. (2007). "Lignin depolymerization/ repolymerization and its critical role for delignification of aspen wood by steam explosion," *Bioresour. Technol.* 98, 3061-3068. DOI: 10.1016/j.biortech.2006.10.018

Manzanares, P., Ballesteros, I., Negro, M. J., Oliva, J. M., González, A., and Ballesteros, M. (2012). "Biological conversion of forage sorghum biomass to ethanol by steam explosion pretreatment and simultaneous hydrolysis and fermentation at high solid content," *Biomass Conv. Bioref.* 2, 123-132. DOI: 10.1007/s13399-012-0040-8

Martínez, A. T., Rencoret, J., Marques, G., Gutiérrez, A., Ibarra, D., Jiménez-Barbero, J., and del Río, J. C. (2008). "Monolignol acylation and lignin structure in some nonwoody plants: a 2D NMR study," *Phytochemistry* 69, 2831-2843. DOI: 10.1016/j.phytochem.2008.09.005

Martínez, A. T., Ruiz-Dueñas, F. J., Martínez, M. J., del Río, J. C., and Gutiérrez, A. (2009). "Enzymatic delignification of plant cell wall: From nature to mill," *Curr. Opin. Biotechnol.* 20, 348-357. DOI: 10.1016/j.copbio.2009.05.002

Martín-Sampedro, R., Capanema, E. A., Hoeger, I., Villar, J. C., and Rojas, O. J. (2011). "Lignin changes after steam explosion and laccase-mediator treatment of eucalyptus wood chips," *J. Agric. Food Chem.* 59, 8761-8769. DOI: 10.1021/jf201605f

Meyermans, H., Morreel, K., Lapierre, C., Pollet, B., De Bruyn, A., Busson, R., Herdewijn, P., Devreese, B., Van Beeumen, J., Marita, J. M., *et al.* (2000). "Modification in lignin and accumulation of phenolic glucosides in poplar xylem upon downregulation of caffeoyl-coenzyme A O-methyltransferase, an enzyme

involved in lignin biosynthesis," *J. Biol. Chem.* 275, 36899-36909. DOI: 10.1074/jbc.M006915200

Miron, J., Zuckerman, E., Sadeh, D., Adin, G., Nikbachat, M., Yosef, E., Ben-Ghedalia, D., Carmi, A., Kipnis, T., and Solomon, R. (2005). "Yield, composition and in vito digestibility of new forage sorghum varieties and their ensilage characteristics," *Anim. Feed. Sci. Technol.* 120, 17-32. DOI: 10.1016/j.anifeedsci.2005.01.008

Morreel, K., Ralph, J., Kim, H., Lu, F. C., Goeminne, G., Ralph, S., Messens, E., and Boerjan, W. (2004). "Profiling of oligolignols reveals monolignol coupling conditions in lignifying poplar xylem," *Plant Physiol.* 136, 3537-3549. DOI: 10.1104/pp.104. 049304

Negro, M. J., Manzanares, P., Ballesteros, I., Oliva, J. M., Cabañas, A., and Ballesteros, M. (2003). "Hydrothermal pretreatment conditions to enhance ethanol production from poplar biomass," *Appl. Biochem. Biotechnol.* 105–108, 87-100. DOI: 10.1007/978-1-4612-0057-4_7

NREL, (2007). "Chemical analysis and testing laboratory analytical procedures," National Renewable Energy Laboratory, Golden, CO (www.1.ere.energy.gov/biomass/analytical_procedures.html).

Prinsen, P., Rencoret, J., Gutiérrez, A., Liitiä, T., Tamminen, T., Colodette, J. L., Berbis, M. A., Jiménez-Barbero, J., Martínez, A. T., and del Río, J. C. (2013). "Modification of the lignin structure during alkaline delignification of eucalyptus wood by kraft, soda-AQ, and soda-O_2 cooking," *Ind. Eng. Chem. Res.* 52, 15702-15712. DOI: 10.1021/ie401364d

Ragauskas, A. J., Beckham, G. T., Biddy, M. J., Chandra, R., Chen, F., Davis, M. F., Davison, B. H., Dixon, R. A., Gilna, P., Keller, M., *et al.* (2014). "Lignin valorization: Improving lignin processing in the biorefinery," *Science* 344(6185), 1246843. DOI: 10.1126/science.1246843

Rahikainen, J. L., Martín-Sampedro, R., Heikkinen, H., Rovio, S., Marjamaa, K., Tamminen, T., Rojas, O. J., and Kruus, K. (2013). "Inhibitory effect of lignin during cellulose bioconversion: The effect of lignin chemistry on non-productive enzyme adsorption," *Bioresour. Technol.* 133, 270-278. DOI: 10.1016/j.biortech.2013.01.075

Ralph, J., Bunzel, M., Marita, J. M., Hatfield, R. D., Lu, F., Kim, H., Schatz, P. F., Grabber, J. H., and Steinhart, H. (2004). "Peroxidase-dependent cross-linking reactions of p-hydroxycinnamates in plant cell walls," *Phytochem. Rev.* 3, 79-96. DOI: 10.1023/B:PHYT.0000047811.13837.fb

Ralph, J., and Landucci, L. L. (2010). "NMR of lignins," *Lignin and Lignans; Advances in Chemistry*, Heitner, C., Dimmel, D. R., and Schmidt, J. A. (eds.), CRC Press, Boca Raton, FL, pp.137-234.

Ralph, J., Marita, J. M., Ralph, S. A., Hatfield, R. D., Lu, F., Ede, R. M., Peng, J., Quideau, S., Helm, R. F., Grabber, J. H., Kim, H., Jimenez-Monteon, G., Zhang, Y., Jung, H.-J. G., Landucci, L. L., MacKay, J. J., Sederoff, R. R., Chapple, C., and Boudet, A. M. (1999). "Solution-state NMR of lignin," in: *Advances in Lignocellulosics Characterization*, Argyropoulos, D. S. (ed.), TAPPI Press, Atlanta, GA, pp. 55-108.

Ralph, S. A., Ralph, J., and Landucci, L. (2004). "NMR database of lignin and cell wall model compounds," USDA Forest Products Laboratory, Madison, WI (http://ars.usda.gov/ Services/docs.htm?docids10491).

Sannigrahi, P., and Ragauskas, A. J. (2011). "Characterization of fermentation residues from the production of bio-ethanol from lignocellulosic feedstocks," *J. Biobased Mat. Bioeng.* 5, 514-519. DOI: 10.1166/jbmb.2011.1170

Samuel, R., Foston, M., Jaing, N., Cao, S., Allison, L., Studer, M., Wyman, C., and Ragauskas, A. J. (2011a). "HSQC (heteronuclear single quantum coherence) 13C–1H correlation spectra of whole biomass in perdeuterated pyridinium chloride–DMSO system: An effective tool for evaluating pretreatment," *Fuel* 90, 2836-2842. DOI: 10.1016/j.fuel.2011.04.021

Samuel, R., Foston, M., Jiang, N., Allison, L., and Ragauskas, A. J. (2011b). "Structural changes in switchgrass lignin and hemicelluloses during pretreatments by NMR analysis," *Polym. Degrad. Stab.* 96, 2002-2009. DOI: 10.1016/j.polymdegradstab.2011.08.015

She, D., Xu, F., Geng, Z.C., Sun, R. C., Jones, G. L., and Baird, M. S. (2010). "Physicochemical characterization of extracted lignin from sweet sorghum stem," *Ind. Crop. Prod.* 32, 21-28. DOI: 10.1016/j.indcrop.2010.02.008

Sun, R. C., Sun, X. F., Wang, S. Q., Zhu, W., and Wang, X. Y. (2002). "Ester and ether linkages between hydroxycinnamic acids and lignins from wheat, rice, rye, and barley straws, maize stems, and fast-growing poplar wood," *Ind. Crop. Prod.* 15, 179-188. DOI: 10.1016/S0926-6690(01)00112-1

Sun, S. L., Wen, J. L., Ma, M. G., Li, M. F., and Sun, R. C. (2013). "Revealing the structural inhomogeneity of lignins from sweet sorghum stem by successive alkali extractions," *J. Agric. Food Chem.* 61, 4226-4235. DOI: 10.1021/jf400824p

Tomás-Pejó, E., Oliva, J. M., and Ballesteros, M. (2008). "Realistic approach for full-scale ethanol production from lignocellulose: A review," *J. Sci. Industrial Res.* 67, 874-884.

Vishtal, A., and Kraslawski, A. (2011). "Challenges in industrial applications of technical lignins," *BioResources* 6(3), 3547-3568. DOI: 10.15376/biores.6.3.3547-3568

Yelle, D. J., Kaparaju, P., Hunt, C. G., Hirth, K., Kim, H., Ralph, J., and Felby, C. (2013). "Two–dimensional NMR evidence for cleavage or lignin and xylan substituents in wheat straw through hydrothermal pretreatment and enzymatic hydrolysis," *Bioenerg. Res.* 6, 211-221. DOI: 10.1007/s12155-012-9247-6

You, T. T., Mao, J. Z., Yuan, T. Q., Wen, J. L., and Xu, F. (2013). "Structural elucidation of the lignins from stems and foliage of *Arundo donax* Linn," *J. Agric. Food Chem.* 61, 5361-5370. DOI: 10.1021/jf401277v

Yuan, T. Q., Sun, S., Xu, F., and Sun, R. C. (2011). "Isolation and physico-chemical characterization of lignins from ultrasound irradiated fast-growing poplar wood," *BioResources* 6, 414-433. DOI: 10.15376/biores.6.1.414-433

Zhou, J. M., and Ibrahim, R. K. (2010). "Tricin – A potential multifunctional nutraceutical," *Phytochem. Rev.* 9, 413-424. DOI: 10.1007/s11101-009-9161-5